Multi-Band-SWIFT

Djaudat Idiyatullin[1], Curtis A. Corum[1], and Michael Garwood[1]
[1]*Radiology, CMRR, University of Minnesota, Minneapolis, MN, United States*

INTRODUCTION The distribution of transverse relaxation times (T_2) in tissues covers about six orders of magnitude, from microseconds (bound water, macromolecules etc.) up to seconds (cerebrospinal fluid, etc.). For diagnostic purposes it is very useful to be able to observe changes of spin density and relaxation parameters due to tissue pathology[1]. This has motivated much interest in MRI methods allowing increased range of detectable short T_2's[2-7]. All of these methods are based on radial readout techniques. To increase the range of detectable short T_2's the excitation and acquisition bandwidths must be increased, along with the strength of readout gradients. For various reasons (e.g., gradient ramp time, RF amplitude, coil ringdown time and SAR), all existing sequences are limited to a maximum achievable bandwidth which may be insufficient to resolve all excited short T_2 signals and to avoid off-resonance artifacts (blurring) in radial imaging. We found that these problems could be reduced by using a DANTE[8] like multiband excitation, which covers a much larger bandwidth while using relatively small average power. To explore this multiband approach we modified the gapped SWIFT (SWeep Imaging with Fourier Transformation)[4, 9] method which allows flexible manipulation of the amplitude and width of the excited sidebands. We call this new method Multi-Band-SWIFT (MB-SWIFT). In contrast to other methods using DANTE-like excitation, for example BURST[10] and its modifications, in MB-SWIFT the acquisition occurs during the excitation, which makes this sequence sensitive to short T_2s. We present here a detailed description of the MB-SWIFT sequence, which yields increased sensitivity and reduced power deposition relative to other methods at high bandwidth and additionally allows analysis of T_2 distributions.

METHODS ***Description of MB-SWIFT pulse sequence*** Fig.1 shows one projection-block of the MB-SWIFT sequence. A stretched hyperbolic secant (*HS*n) frequency-modulated pulse[11] is used. Only the gradient orientation is changed from projection to projection. In contrast to the original SWIFT pulse, here we use fewer gaps, N_G, and greatly reduce the transmitter duty cycle $d_c = \tau_p b_w$, where b_w is the width of the nominal baseband and τ_p is the duration of sub-pulse elements. In addition we utilize a higher oversampling value, N_{OS}, which is equal to number of samples in each gap. In the simplest version of MB-SWIFT, b_w is matched to the linear width (in frequency units) of the voxel, and N (number of sidebands) will cover the diameter of the spherical FOV. The gapped excitation creates sidebands with amplitudes $A_m = \mathrm{sinc}(md_c)$, where m is the sideband order[9] and the width of the sideband is equal to or smaller than b_w. Sideband width is governed by the amplitude of the frequency-modulation parameter, σ, in the range $0 \le \sigma \le b_w/2$. The fraction of the excited part of a voxel, p, is determined by $p=(2\sigma N_G/b_w+1)/N_G$. The smallest excited fraction is then bounded by $1/N_G$ when $\sigma = 0$. For steady-state imaging, it is important to keep the excitation profile as uniform as possible throughout the FOV[12]. To reach 5% falloff at the edges of the FOV, the τ_p should be chosen as $\tau_p=1/(3Nb_w)$[9, 13]. In this case the maximum sideband order is equal to $m_{max}=\mathrm{int}(1/(6d_c))$. After acquisition the signal is Fourier transformed (FT) and correlated with the pulse function as in the original SWIFT method[4]. In contrast to SWIFT data, MB-SWIFT data is averaged in the frequency (projection) domain (after phasing) for each excited band (stripe) area to yield one data point (in simplest case) per stripe along the projection. Subsequently the FT of the down-sampled projection data is the desired spoke in k-space. Missing time domain points (under the transmitted pulse) are estimated using an SVD method[14]. After this procedure, the down-sampled k-space data are reconstructed by gridding[15]. Simulated MB-SWIFT data and the corresponding stripe-averaged projection of a stepped object are presented in Fig. 2.

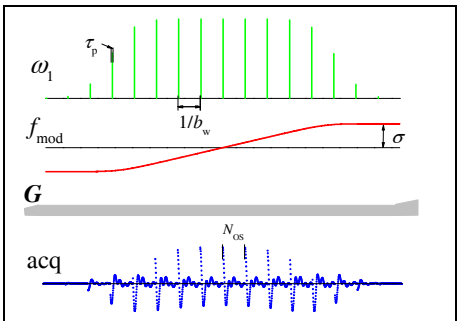

Fig.1. Schematic of one projection-block of the MB-SWIFT sequence with HS4 type frequency modulated pulse.

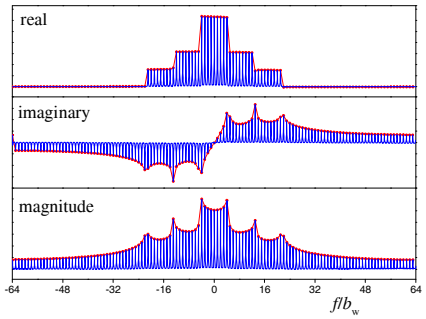

Fig.2. Simulated MB-SWIFT data using a stepped object and 128 sidebands (blue line), and down-sampled data (red line and circles).

SAR and SNR The peak RF amplitude needed for excitation to a flip angle □ in the bandwidth pb_w, using a gapped chirp pulse (for simplicity) can be approximated by $\omega_{1max} \approx 3s_w\theta\sqrt{p/N_G}$, which for striped excitation is a factor $\sqrt{p/N_G}$ times less in comparison with a square pulse[9] (e.g. for a ZTE[16] sequence) using the same excitation spectral width equal to $s_w=b_wN_{OS}$. In comparison with N_G-times signal-averaged ZTE using the optimized (Ernst angle) steady-state condition, MB-SWIFT requires about $(N_G + 1 + 2\sqrt{N_G})/4$ - times reduced SAR, while yielding the same SNR for the case of p=1; for the case of $p=1/N_G$ using the same power, SNR increases by $(N_G + 1)/(2\sqrt{N_G})$. Thus the MB-SWIFT sequence allows flexibility for optimizing the specific experimental conditions. Due to coherence build up during excitation, MB-SWIFT has different sensitivity to homogeneous and inhomogeneous broadening of the signal. This can be used for extracting the T_2^* distribution in a single scan experiment. The images presented here were acquired at 9.4T (Agilent) by using a chirp pulse (for MB-SWIFT) with N_G=16, N_{OS}=128 and $p=1/N_G$.

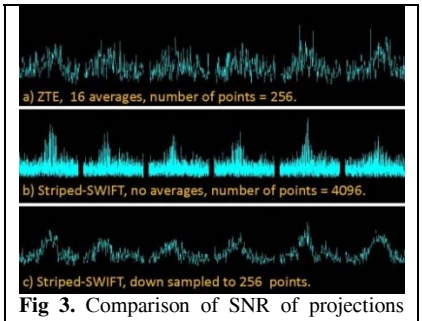

Fig 3. Comparison of SNR of projections acquired with low flip angle using ZTE with N_G signal averages (a) and MB-SWIFT with N_G=16 (b,c) at 500kHz. Other parameters were fixed for imaging this water phantom.

RESULTS and DISCUSSION Fig.3 presents a comparison of SNR at low flip angle for N_G-times averaged ZTE and MB-SWIFT projections at 500kHz with N_G=16 and similar other parameters. These results show an approximate two-fold higher SNR for MB-SWIFT, which is predicted theoretically. As an example of the advantage of higher bandwidth, Fig.3 presents bone images without fat saturation in the presence of a brass screw. Highly blurred images at 100kHz become sharp with 500kHz bandwidth.

CONCLUSION The MB-SWIFT sequence shows increased sensitivity and lower power deposition relative to other methods at extremely high excitation and acquisition bandwidths and allows analysis of the homogeneous and inhomogeneous contribution to T_2^*. The method could find application in many areas including materials science and medical imaging. Specifically, we expect that this method could be most effectively used for imaging objects with inhomogeneously broadened signals, as for example lung or tissues next to metallic implants.

Acknowledgements This research supported by NIH P41 EB015894, P41-RR008079-19S1, S10-RR023730, S10-RR027290 S10-RR008079, R21-CA139688 grants and WM Keck Foundation. **References** 1Bydder EMR 2012; 2Bergin Radiol 1991; 3Gatehouse ClinRadiol 2003; 4Idiyatullin JMR 2006; 5Hafner MRI 1994; 6Madio MRM 1995; 7Weiger MRM 2011; 8Morris JMR 1978; 9Idiyatullin JMR 2008; 10Hennig *MAGMA* 1993; 11Garwood JMR 2001; 12Garwood EMR 2012; 13Kunz MRM 1986; 14Kuethe JMR 1999; 15Jackson MedImag 1991; 16Weiger MRM 2013.

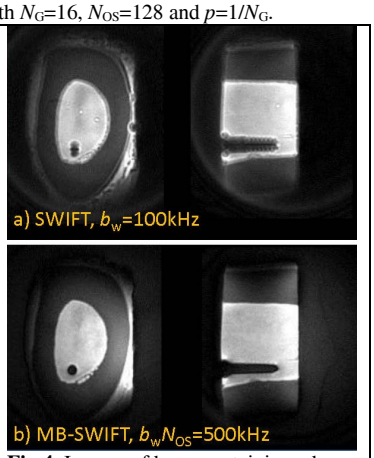

Fig 4. Images of bone containing a brass screw, acquired using regular SWIFT at 100kHz (a) and MB-SWIFT at 500kHz (b), using the same (2.5min) scan time.